Kinematic Analysis of a Two-Link Object for Whole Arm Manipulation

ZAKARYA ZYADA, YOSHIKAZU HAYAKAWA and SHIGEYUKI HOSOSE
RIKEN-TRI Collaboration Center for Human-Interactive Robot Research,
Nagoya Science Park, 2271-130 Anagahora, Shimoshidami, Moriyama-ku, Nagoya, Aichi 463-0003, JAPAN
{zzyada, hayakawa and hosoe}@nagoya.riken.jp, http://rtc.nagoya.riken.jp/index-e.html

Abstract: - This paper presents kinematic analysis of free-ended two-rigid-links object manipulated by two arms as an initial step simplification towards the analysis of holding and manipulating a human body by a humanoid robot. Rolling as well as sliding at the points of contact of the two-links object constrained by the holding two-arms is explained. Position, velocity and acceleration analysis of the manipulated object, position, velocity and acceleration constraints as well as expressions for sliding displacement, sliding velocity and sliding acceleration are presented. Simulation results for links sliding acceleration, the object joint acceleration and object configurations for different input rolling accelerations are presented. The presented position, velocity and acceleration analysis proves that: 1- through manipulating two-links object by two-arms, rolling about one arm or both arms at the points of contact is associated with sliding at both points of contact. There is no rolling without sliding and there is no sliding without rolling. 2- It is possible to define the object links velocities or accelerations as well as sliding accelerations from the contact rolling velocities and accelerations estimations or measurements. 3- It is possible to define the configuration of the object from contact points and hence contact angle measurements, applying tactile sensors.

Key-Words: - Kinematics analysis, whole arm manipulation, dynamic manipulation, cooperative manipulation, rigid body, position analysis and velocity analysis.

1 Introduction

Nursing robotics have received a considerable attention by different research groups seeking their promising human-friendly assist and cooperation. Among these groups is RIKEN-TRI robotics research group who introduced RI-MAN for holding and transferring a patient, [1], [2]. RI-MAN is designed to grasp, hold and transfer a human applying its whole two-arms, Fig. 1. Whole arm manipulation is an approach to manipulation that employs all the available manipulation surfaces of the robot to act upon and sense the environment, [3]. Restraining large size objects, lifting heavy loads or assembling mating parts are examples of suitable tasks that require whole arm manipulation. Whole arm grasps are formed by wrapping the arms (or fingers) around the objects, [4]. Manipulating a human, (the target is a patient), as shown in Fig. 1, lies in the taxonomy of dynamic manipulation in which task dynamics is significant for analysis and planning. Kinematic, static and quasi-static manipulation analysis are important steps for dynamic manipulation. Dynamic manipulation has many benefits such as increasing the repertoire of actions to manipulators, increasing the speed of manipulation and saving the complexity and the

Fig. 1. RI-MAN holding a dummy patient, [2]

mass of the robot, [5]. With dynamic manipulation, some of the complexity of the robot system is transferred from the hardware (joints and actuators) to planning and control, [6]. Many research works for different dynamic manipulation tasks can be found in the literature. Motion planning of a 1-DOF dynamic pitching robot throwing a ball in a horizontal plane is presented in [7]. Dynamic manipulation of an object over a plate inspired by the handling of a pizza peel is presented in [8]. Motion planning and controllability for non-prehensile (without a form- or force-closure) manipulation for throwing and catching a disc using two planar manipulators are presented in [9].

Carrying a polygonal shape object applying two mobile robots with non-prehensile manipulators has been presented in [10]. So far the presented work is concerned with one-link object to be manipulated by one or two manipulators. However an application like holding and/or transferring a human, (patient for instance), is an example of multi-link object which is not tackled in research literature, (up to the authors' knowledge), in robotics manipulation. To define, apply and assure stable holding and manipulating as well as control, it is important to analyze and understand kinematics and dynamics of the manipulated multi-link object. As an initial step towards analysis of holding and manipulating a human body object, this paper introduces two-dimensional position, velocity and acceleration analysis of free ended two-link rigid body object hold by two arms, Fig. 3. Kinematic relations as well as kinematic constraints are to be introduced. Through analysis and simulation, it is aimed to answer the following questions:

Given the acceleration of rolling around the points of contact, (defined by θ_1 and θ_2 in Fig. 3), for a two-link object hold by two-arms, at any instant: a) Is it possible to get information about object-joint acceleration, velocity and position?, b) Is it possible to get information about the sliding accelerations, velocities and amount of sliding of links over arms?, c) How are links sliding motions (acceleration, velocity and position) associated with rolling motions (acceleration, velocity and position) ?, d) Is it possible to get information about the object configuration?

This paper is organized as follows: rolling and sliding of one link object over one arm in a plane is presented in section II. Position analysis of two-link object constrained by two-arms with rolling and sliding motions, position constraints, sliding displacement expressions and position simulation results are introduced in section III. Velocity analysis of two-link object constrained by two-arms, velocity constraints, sliding velocity expressions are introduced in section IV. Acceleration analysis of two-link object constrained by two-arms, acceleration constraints, sliding acceleration expressions and the acceleration simulation results for different rolling accelerations are introduced in section V. Conclusion and directions for future work are to be presented in section VI.

2. Rolling and Sliding of One Link Object

In this section, rolling and/or sliding of a slim rigid-link object over a rigid-link arm system, Fig. 2, is explained. Contact type is assumed to be hard contact. The coordinate system is introduced first followed by explanation of the different possible rolling and/or sliding motions.

2.1 Coordinate system

The coordinate system is defined as shown in Fig. 2. A reference coordinate frame 0, $O_0 - x_0y_0$ is defined at the center of the circular cross section of the arm; two frames S_{1l} and S_{1c} both initially having the origin at the point of contact between the link and the arm, s_1, are also defined. Frame S_{1l}, $(O_{1l} - x_{1l}y_{1l})$, is fixed to the link while frame S_{1c}, $(O_{1c} - x_{1c}y_{1c})$, is at the point of contact between the link and the arm; x_{1c} is in the dirction of line from O_0 to s_1 which is also normal to the plane including the point of contact as shown in Fig. 2. Frame e, $O_e - x_ey_e$ is attached to the right end of the arm. The angle θ_1, denoted as the angle of contact, is measured from x_0 to x_{1c} and being positive counter clockwise; the length l_1 expresses link segment length from the origin of frame S_{1c} to the origin of frame e. The total length of the object link is a_1; Clearly l_1 is a variable while a_1 is a constant.

The rolling and/or sliding motion between the link object and the arm can be clarified in terms of the relative position of the two reference frames S_{1l} and S_{1c} before and after the motion. After a motion of rolling and/or sliding, frames S_{1l} and S_{1c} are denoted by $S_{1l}^{'}$ and $S_{1c}^{'}$ respectively. Knowing the initial angle of contact $\theta_1(0)$ and the initial length $l_1(0)$ and defining the motion, (rolling and/or sliding), the change in angle of contact $\Delta\theta_1$ and the change in length Δl_1 can be defined. To explain the motions, three cases are considered: 1) sliding of the link over the arm (without rolling); 2) rolling of the link over the arm (without sliding); and 3) both sliding and rolling of the link over the arm.

2.2 Sliding (without rolling)

Assuming that the link has the possibility to slide (without rolling) over arm, then the contact point after sliding will remain at its location before sliding, ($S_{1c}^{'}$ will be identical to S_{1c}). Hence the angle of contact after sliding, θ_1, will be equal to the initial angle of contact, $\theta_1(0)$, then

$$\Delta\theta_1 = \theta_1 - \theta_1(0) = 0 \quad (1)$$

Moreover the frame on the link side S_{1l} as well as the whole link will move according to the amount of sliding displacement, d_1. S_{1l} will become in a new

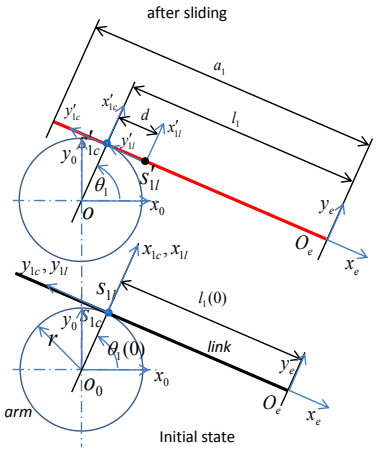

(a)

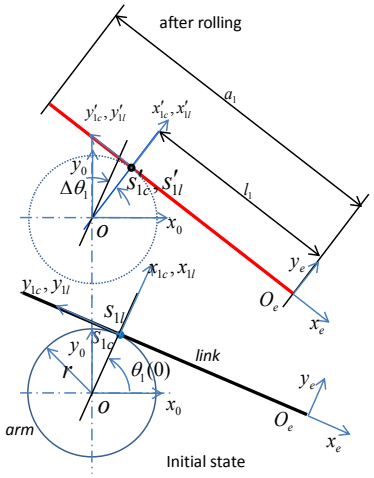

(b)

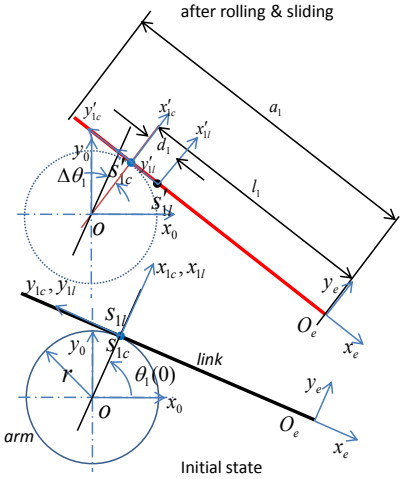

(c)

Fig. 2. Graphical representation of rolling and/or sliding motion of a link over an arm, (lower graph: before motion; upper graph: after motion); (a) sliding motion only, (b) rolling motion only, (c) both rolling and sliding motion.

position S'_{1l}. The length l_1 after sliding, will depend on its initial length, $l_1(0)$, and amount of sliding d_1.

$$\Delta l_1 = l_1 - l_1(0) = d_1 \quad (2)$$

2.3 Rolling (without sliding)

Assuming that the link has the possibility to roll without sliding, then both S_{1c} and S_{1l} will be identical and move on the circle of radius r, (the peripheral of the arm), with the amount of rolling distance, $r\Delta\theta_1$, to another position denoted by S'_{1c} and S'_{1l}. The change in the angle of contact $\Delta\theta_1$ is a function of the angle of contact after rolling, θ_1, and the initial angle of contact, $\theta_1(0)$,

$$\Delta\theta_1 = \theta_1 - \theta_1(0) \quad (3)$$

The change in length because of rolling can be defined as:

$$\Delta l_1 = l_1 - l_1(0) = -r\Delta\theta_1 \quad (4)$$

2.4 Sliding and rolling

Assuming that the link has the possibility to slide and to roll, then both S_{1c} and S_{1l} will move to different new positions according to rolling angle and sliding displacement. S_{1c} will become S'_{1c} according to amount of roll, $r\Delta\theta_1$, while S_{1l} become S'_{1l} according to the amount of sliding, d_1. The new length l_1 will depend on $r\Delta\theta_1$ as well as d_1 and the initial length $l_1(0)$. Expressions for change in the angle of contact and the change in length will be the summation of both the sliding case and the rolling case;

$$\Delta\theta_1 = \theta_1 - \theta_1(0) \quad (5)$$

The change in length because of both sliding and rolling can be defined as:

$$\Delta l_1 = l_1 - l_1(0) = d_1 - r\Delta\theta_1 \quad (6)$$

3. Position Analysis of Constrained Two-Link Object

Understanding the kinematics and dynamics of the human body as an object manipulated by the whole arms of a humanoid robot is important for stable manipulation and control. As an initial step simplification towards this difficult problem, the author considers a two-dimensional system of two slender-rigid-link object constrained by two-arms as shown in Fig. 3. In this section position analysis is presented. Sliding and/or rolling motion of two-rigid-link object constrained by two arms is to be presented.

The object is a two free-ended rigid-links, (link 1 and link 2), with total lengths a_1 and a_2 connected with a

passive revolute joint. The two-link object is constrained by two arms, (right and left arms). Link 1 has a point contact with the cylindrical right-arm at s_1 while link 2 has a point contact with the cylindrical left-arm at s_2. For the purpose of analysis, the base coordinate frame, (frame b), $o_b - x_b y_b$, the right arm coordinate frame, (frame r), $o_r - x_r y_r$, left-arm coordinate frame, (frame l), $o_l - x_l y_l$, contact points coordinate frames, (frame s_1), $o_{s_1} - x_{s_1} y_{s_1}$ and (frame s_2), $o_{s_2} - x_{s_2} y_{s_2}$, (frame 3), $o_3 - x_3 y_3$ are defined as shown in Fig. 3. The angles of contact, θ_1 is the angle from the x-axis of frame b to the x-axis of frame s_1 while the angle of contact θ_2 is the angle from the x-axis of frame b to the x-axis of frame s_2, Fig. 3, both being positive in a counter clockwise sense. l_1 and l_2 define link segment lengths from origins of frames s_1 and s_2 at the points of contact to the passive joint, origin of frame 3, respectively. It is aimed to get for a two-link manipulated object, constrained as shown in Fig. 3, the constraining relation between l_1, l_2 and θ_1, θ_2.

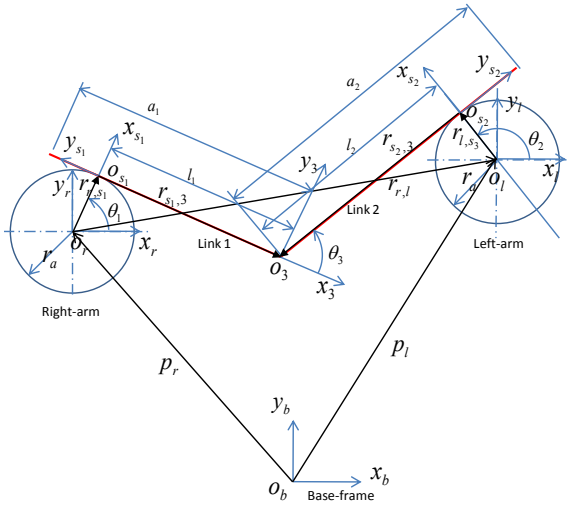

Fig. 3. Coordinate systems of free-ended two-link object by constrained by two-arms

3.1 Position of passive joint 3

The position of the passive joint, frame 3, through the right-arm branch, can be described as:

$$p_3^b = p_r^b + r_{r,s_1}^b + R_{s_1}^b r_{s_1,3}^{s_1} \quad (7)$$

where p_r^b is the position vector from the origin of frame b to the origin of frame r expressed in frame b; r_{r,s_1}^b is the position vector from origin of frame r to origin of frame s_1 expressed in frame b; $r_{s_1,3}^{s_1}$ is the position vector from origin of frame s_1 to the origin of frame 3 expressed in frame s_1; and $R_{s_1}^b$ is the rotation matrix from frame s_1 to frame b.

3.2 Constrained sliding and rolling:

In a similar way, the position of the passive joint, frame 3, through the left-arm branch, can be described as:

$$p_3^b = p_l^b + r_{l,s_2}^b + R_{s_2}^b r_{s_2,3}^{s_2} \quad (8)$$

where p_l^b is the position vector from the origin of frame b to the origin of frame l expressed in frame b; r_{l,s_2}^b is the position vector from origin of frame l to the origin of frame s_2 expressed in frame b; $r_{s_2,3}^{s_2}$ is the position vector from the origin of frame s_2 to the origin of frame 3 expressed in frame s_2; $R_{s_2}^b$ is the rotation matrix from frame s_2 to frame b. The relative position of the two arms can be expressed as:

$$p_l^b = p_r^b + R_r^b r_{r,l}^r \quad (9)$$

where $r_{r,l}^r$ is the position vector from the origin of frame r to

the origin of frame l expressed in frame r; and R_r^b is the rotation matrix from frame r to frame b. Substituting (9) into (8) and equalizing (8) and (7), then

$$r_{r,s_1}^b + R_{s_1}^b r_{s_1,3}^{s_1} = R_r^b r_{r,l}^r + r_{l,s_2}^b + R_{s_2}^b r_{s_2,3}^{s_2} \quad (10)$$

from which, the following constraint equation can be derived,

$$\begin{bmatrix} s\theta_1 & s\theta_2 \\ -c\theta_1 & -c\theta_2 \end{bmatrix} \begin{bmatrix} l_1 \\ l_2 \end{bmatrix} + \begin{bmatrix} x_{r,l} - r_a(c\theta_1 - c\theta_2) \\ y_{r,l} - r_a(s\theta_1 - s\theta_2) \end{bmatrix} = \begin{bmatrix} 0 \\ 0 \end{bmatrix} ; \quad (11)$$

where $s\theta_i = sin(\theta_i)$; $c\theta_i = cos(\theta_i)$; $x_{r,l}$ and $y_{r,l}$ are the components of position vector $r_{r,l}^r$ in x and y directions respectively; r_a is the radius of both right-arm and left-arm cross section.

3.3 Configuration determination from tactile sensors measurements

Determination of the configuration of the manipulated object is important in dynamic manipulation planning and control. Human do that applying his vision as well as his skin force/position sensors. According to the constraint equation (11), it is possible to define the configuration from tactile sensor measurements. Constraint equation (11) defines the lengths l_1, l_2 in terms of the contact angles θ_1, θ_2 and the relative position of the two-manipulating arms. For given arm size, r_a, relative position, $r_{r,l}^r$, of the two-arms; if it possible to measure (or estimate) the angles of contact θ_1 and θ_2, it is possible to determine the lengths l_1, l_2 which completely define the configuration of the constrained two-links object. Constraint equation (11) clarifies that if roll happens, the configuration will

change. Also, in another way, if the configuration of the object is changed, the angles of contact will be changed. Measurements of the angles of contact can be obtained through the tactile sensors proposed by another research team in our institute for the humanoid robot RI-MAN, [11].

3.4 Rolling-sliding relation

It is important to define the sliding-rolling relation for future study of planning and control for the current problem of dynamic manipulation. As shown in section II, (equation 6), sliding, d_i, is a function of the change in angle of contact, $\Delta\theta_i$ and the change in length Δl_i for any two system states. The amount of sliding, d_i (referred to the frame s_i), can be expressed as:

$$\begin{Bmatrix} d_i = \Delta l_i + r\Delta\theta_i;\ i = 1 \\ d_i = \Delta l_i - r\Delta\theta_i;\ i = 2 \end{Bmatrix} \quad (12)$$

Given the angles of contact $\theta_i, (i = 1,2)$, (and hence the lengths $l_i, (i = 1,2)$, from equation 11), for any two different instants, the change in length Δl_i, and the change in angle of contact $\Delta\theta_i$ can be obtained, from which the amount of sliding $d_i, (i = 1,2)$, can be estimated at both points of contact. Equation (12) assures that for manipulating two-links by two-arms both rolling and sliding are associated with each other. If roll happened over one or the two arms, sliding at the contact points exist. If sliding at the contact points happened, roll also exists at one or two of contact points. So, if the amount of roll is defined, (as it can be estimated through tactile sensor measurements), the sliding can be defined by (12).

4. Velocity Analysis of Constrained Two-Link Object

In this section, the analysis of two-link object constrained by two-arms is extended to include object links' velocities. The velocity of the passive joint, the velocity constraint equation and the sliding velocity expressions are introduced.

4.1 Velocity of passive joint 3

Differentiating the position equation (7), the velocity of the passive joint can be obtained,

$$\dot{p}_3^b = \dot{p}_r^b + \dot{r}_{r,s_1}^b + \dot{R}_{s_1}^b r_{s_1,3}^{s_1} + R_{s_1}^b \dot{r}_{s_1,3}^{s_1} \quad (13)$$

Substituting with the individual components, then

$$\begin{bmatrix} \dot{p}_{3x}^b \\ \dot{p}_{3y}^b \end{bmatrix} = \begin{bmatrix} \dot{p}_{rx}^b \\ \dot{p}_{ry}^b \end{bmatrix} + \begin{bmatrix} -r_a s\theta_1 - l_1 c\theta_1 & -s\theta_1 \\ r_a c\theta_1 - l_1 s\theta_1 & c\theta_1 \end{bmatrix} \begin{bmatrix} \dot{\theta}_1 \\ \dot{l}_1 \end{bmatrix} \quad (14)$$

4.2 Velocity constraint equation

The velocity constraint equation can be obtained by differentiating equation (11) as:

$$\begin{bmatrix} s\theta_1 & s\theta_2 \\ -c\theta_1 & -c\theta_2 \end{bmatrix} \begin{bmatrix} \dot{l}_1 \\ \dot{l}_2 \end{bmatrix} + \begin{bmatrix} r_a s\theta_1 + l_1 c\theta_1 & -r_a s\theta_2 + l_2 c\theta_2 \\ -r_a c\theta_1 + l_1 s\theta_1 & r_a c\theta_2 + l_2 s\theta_2 \end{bmatrix} \begin{bmatrix} \dot{\theta}_1 \\ \dot{\theta}_2 \end{bmatrix} + \begin{bmatrix} \dot{x}_{r,l} \\ \dot{y}_{r,l} \end{bmatrix} = \begin{bmatrix} 0 \\ 0 \end{bmatrix} \quad (15)$$

4.3 Sliding velocity estimation

Differentiating equation (12), sliding velocity $\dot{d}_i$ can be obtained as a function of velocity of *i*th link, $\dot{l}_i$ and *i*th rolling velocity, $\dot{\theta}_i$ as follows:

$$\begin{Bmatrix} \dot{d}_i = \dot{l}_i + r\dot{\theta}_i;\ i = 1 \\ \dot{d}_i = \dot{l}_i - r\dot{\theta}_i;\ i = 2 \end{Bmatrix} \quad (16)$$

Estimating the velocities of rolling $\dot{\theta}_1, \dot{\theta}_2$, the velocities of links, $\dot{l}_1, \dot{l}_2$, and sliding velocities $\dot{d}_1, \dot{d}_2$, can be estimated.

5. Acceleration Analysis of Constrained Two-Link Object

In this section, the analysis is extended to include object links' accelerations. The acceleration of the passive joint, the acceleration constraint equation and the sliding acceleration expressions as well as simulation results are introduced.

5.1 Acceleration of passive joint 3

Differentiating the velocity equation (14), the acceleration of the passive joint can be obtained as,

$$\begin{bmatrix} \ddot{p}_{3x}^b \\ \ddot{p}_{3y}^b \end{bmatrix} = \begin{bmatrix} \ddot{p}_{rx}^b \\ \ddot{p}_{ry}^b \end{bmatrix} + \begin{bmatrix} -r_a s\theta_1 - l_1 c\theta_1 & -s\theta_1 \\ r_a c\theta_1 - l_1 s\theta_1 & c\theta_1 \end{bmatrix} \begin{bmatrix} \ddot{\theta}_1 \\ \ddot{l}_1 \end{bmatrix} + \begin{bmatrix} -r_a c\theta_1 + l_1 s\theta_1 & -2c\theta_1 \\ -r_a s\theta_1 - l_1 c\theta_1 & -2s\theta_1 \end{bmatrix} \begin{bmatrix} \dot{\theta}_1^2 \\ \dot{\theta}_1 \dot{l}_1 \end{bmatrix} \quad (17)$$

5.2 Acceleration constraint equation

In a similar way, differentiating the velocity constraint equation (15), will lead to the acceleration constraint equation as,

$$\begin{bmatrix} s\theta_1 & s\theta_2 \\ -c\theta_1 & -c\theta_2 \end{bmatrix} \begin{bmatrix} \ddot{l}_1 \\ \ddot{l}_2 \end{bmatrix} + 2 \begin{bmatrix} c\theta_1 & c\theta_2 \\ s\theta_1 & s\theta_2 \end{bmatrix} \begin{bmatrix} \dot{\theta}_1 \dot{l}_1 \\ \dot{\theta}_2 \dot{l}_2 \end{bmatrix} + \begin{bmatrix} r_a s\theta_1 + l_1 c\theta_1 & -r_a s\theta_2 + l_2 c\theta_2 \\ -r_a c\theta_1 + l_1 s\theta_1 & r_a c\theta_2 + l_2 s\theta_2 \end{bmatrix} \begin{bmatrix} \ddot{\theta}_1 \\ \ddot{\theta}_2 \end{bmatrix} +$$

$$\begin{bmatrix} r_a c\theta_1 - l_1 s\theta_1 & -r_a c\theta_2 - l_2 s\theta_2 \\ r_a s\theta_1 + l_1 c\theta_1 & -r_a s\theta_2 + l_2 c\theta_2 \end{bmatrix} \begin{bmatrix} \dot{\theta}_1^2 \\ \dot{\theta}_2^2 \end{bmatrix} + \begin{bmatrix} \ddot{x}_{r,l} \\ \ddot{y}_{r,l} \end{bmatrix} = \begin{bmatrix} 0 \\ 0 \end{bmatrix} \quad (18)$$

5.3 Sliding acceleration estimation

Differentiating equation (16), sliding acceleration $\ddot{d}_i$ can be obtained as a function of the acceleration $\ddot{l}_i$ and rolling acceleration, $\ddot{\theta}_i$ as follows:

$$\left.\begin{matrix} \ddot{d}_i = \ddot{l}_i + r\ddot{\theta}_i;\ i = 1 \\ \ddot{d}_i = \ddot{l}_i - r\ddot{\theta}_i;\ i = 2 \end{matrix}\right\} \quad (19)$$

5.4 Acceleration Simulation Results

The presented governing equations for position, velocity and acceleration analysis as well as position and velocity constraints are simulated through an implemented MATLAB program. Because of the limited space, it is presented here the simulation results of acceleration and acceleration constraints only. The independent input variables are the rolling accelerations, ($\ddot{\theta}_1$ and $\ddot{\theta}_2$), and initial velocities ($\dot{\theta}_1(0)$ and $\dot{\theta}_2(0)$) and initial positions, ($\theta_1(0)$ and $\theta_2(0)$). The rolling accelerations are assumed as a nonlinear function of time; the rolling velocities $\dot{\theta}_1$, $\dot{\theta}_2$ and the rolling angles θ_1 and θ_2 are obtained through simple integration. The sampling time is assumed to be 0.01 s. the relative velocity of the arms is assumed zero. In real time implementation, the angles of contact can be obtained from tactile sensor measurements and the rolling velocity and accelerations, can be estimated.

The simulation results are shown in Fig. 4. The relative acceleration, $\ddot{l}_1$, sliding velocity, $\ddot{d}_1$, (of link1 over the right-arm at the point of contact, s_1), and the linear velocity, $r_a\ddot{\theta}_1$, (due to a rolling acceleration, $\ddot{\theta}_1$, of link 1 over the right-arm), are shown in Fig. 4a. Similarly, the relative acceleration, $\ddot{l}_2$, sliding acceleration, $\ddot{d}_2$, (of link 2 over the left-arm at the point of contact, s_2), and the linear acceleration, $r_a\ddot{\theta}_2$, (due to a rolling acceleration, $\ddot{\theta}_2$, of link 2 over the left-arm), are shown in Fig. 4b. These two figures, 4a and 4b assure that: 1- if there is rolling then there is associated sliding; it can be said for a two free ended object manipulated by two whole arms; there no rolling without sliding and there is no sliding without rolling; both are associated with each other; 2- if it is possible to estimate the acceleration (or velocity) of rolling, it is possible to estimate the object joint relative accelerations (or velocities) as well as the sliding accelerations (velocities); also if it is possible to estimate the joint relative accelerations (velocities). It is possible to estimate the rolling velocities (and/or accelerations) using tactile sensor measurements; 3- as a result it is possible to estimate the amount of sliding and of the amount of link motion. Also, equations (11, 12) have the same interpretation. Fig. 4c presents the acceleration of the passive joint 3 while Fig. 4d presents some configurations of the object. The presented configurations are the results of positions analysis simulations from equation (11). If the points of contact are measurable, (applying tactile sensor), and hence the angles of contact, then the lengths from the points of contact to the passive joint are definable which completely define the configuration. Fig. 4c and Fig. 4d show that not only object configuration is detectable but also the object joints' accelerations (velocities) which are important for future dynamic manipulation planning and control.

6. Conclusion

Kinematic analysis and acceleration simulation results of free-ended two-link object motion hold by two arms are presented. The main conclusions derived from the presented research work can be summarized as: 1- for dynamic manipulation of two-link object by two arms, rolling of a link about an arm is associated with sliding of the link over the arm at the point of contact. There is no rolling without sliding and there is no sliding without rolling; 2- through the measurements of contact points and hence the angles of contact, applying a tactile sensor, the configuration of the manipulated two-link object can be determined; 3- through estimating the rolling accelerations (velocities), joint relative accelerations (velocities) and hence the sliding accelerations (velocities) at both points of contact can be estimated.

Future Work

For dynamic analysis and control, it important to analyze forces including gravity forces and friction forces at the points of contact. It is also important to define stable manipulation and to control object sliding. So, force analysis as well as sliding control for stable manipulation will be of future interest.

References

[1] T. Odashima, M. Onishi, K. Tahara, T. Mukai, S. Hirano, Z. Luo and S. Hosoe, Development and Evaluation of a Human-interactive Robot Platform

"RI-MAN", *Journal of Robotics Society of Japan*, vol. 25, No. 4, 2007, pp. 554–565.

[2] M. Onishi, Z. Luo, T. Odashima, S. Hirano, K. Tahara and T. Mukai, Generation of Human Care Behaviors by Human-Interactive Robot "RI-MAN", *IEEE International Conference on Robotics and Automation*, 2007, pp. 3128–3129.

[3] K. Salisbury, W. Townsend, B. Ebrman and D. DiPietro, Preliminary Design of a Whole-Arm Manipulation System (WAMS), *IEEE International Conference on Robotics and Automation*, 1988, pp. 254–260.

[4] P. Song, M. Yashima and V. Kumar, Dynamics and Control of Whole Arm Grasps, *IEEE International Conference on Robotics and Automation*, 2001, pp. 2229–2234.

[5] M. Mason and K. Lynch, Dynamic Manipulation, *Proc. Of the 1993 IEEE/RSJ International Conference on Intelligent Robots and Systems*, 1993, pp. 152–159.

[6] K. Lynch and M. Mason, Dynamic Underactuated Nonprehensile Manipulation, *Proceedings of the 2006 IEEE International Conference on Intelligent Robots and Systems*, 2006, pp. 889-896.

[7] W. Mori, J. Ueda and T. Ogasawara, 1-DOF Dynamic Pitching Robot that Independently Controls Velocity, Angular velocity, and Direction of a Ball: Contact Models and Motion Planning, *IEEE International Conference on Robotics and Automation*, 2009, pp. 1655–1661.

[8] M. Higashimori, K. Utsumi, Y. Omoto and M. Kaneko, Dynamic Manipulation Inspired by the Handling of a Pizza Peel, *IEEE Transactions on Robotics*, Vol. 25, No.4, 2009, pp. 829-838.

[9] B. Beigzadeh, M. Ahmadabadi and A. Meghdari, Two Dimensional Dynamic Manipulation of a Disc Using Two Manipulators, *Proceedings of the 2006 IEEE International Conference on Mechatronics and Automation*, 2006, pp. 1191-1196.

[10] A. Gupta and W. Huang, A Carrying Task for Nonprehensile Mobile Manipulators, *Proceedings of the 2003 IEEE/RSJ International Conference on Intelligent Robots and Systems*, 2003, pp. 2896-2901.

[11] T. Mukai, M. Onishi, T. Odashima, S. Hirano, and Z. Luo, Development of the Tactile Sensor System of a Human-Interactive Robot "RI-MAN", *IEEE Transactions on Robotics*, Vol. 24, No.2, 2008, pp. 505-512.

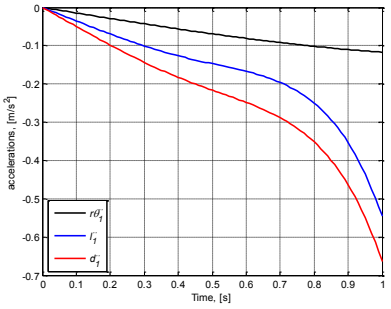

a) roll linear acceleration, joint relative acceleration and sliding acceleration of link 1 over right-arm.

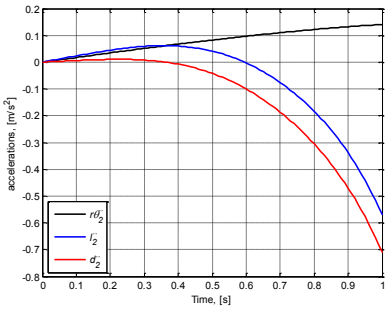

b) roll linear acceleration, joint relative acceleration and sliding acceleration of link 2 over left-arm.

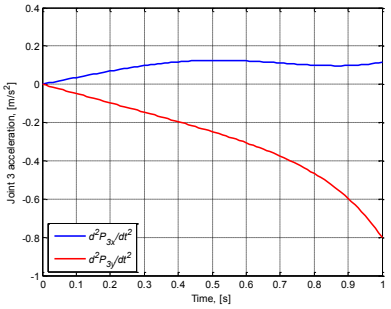

c) acceleration components of the passive joint 3

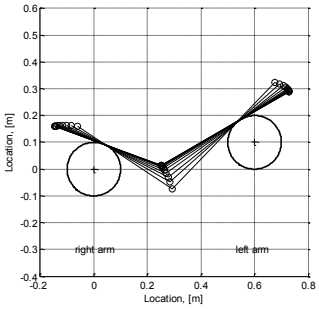

d) configurations changes

Fig. 4. Simulation results of free-ended two-link object constrained by two-arms for rolling around the respective arms at both s1 and s2.